Electronic Supplementary Material (ESI) for Chemical Communications
This journal is © The Royal Society of Chemistry 2012

Supporting Information for:

Probing the redox non-innocence of Co(II) nindigo complexes: not simply β–diketiminate variants

Skye Fortier,[a] Octavio González-del Moral,[a] Chun-Hsing Chen,[a] Maren Pink,[a] Jennifer J. Le Roy,[b] Muralee Murugesu,[b] Daniel J. Mindiola,*[a] and Kenneth G. Caulton*[a]

[a]*Department of Chemistry, Indiana University, 800 E. Kirkwood Avenue, Bloomington, Indiana, USA.*
[b]*Department of Chemistry, University of Ottawa, Ottawa, ON KIN6N5, Canada*

Table of Contents

This journal is © The Royal Society of Chemistry 2012

General Considerations. All air and moisture sensitive operations were performed in an M. Braun Lab Master dry box under an atmosphere of purified nitrogen or using high vacuum standard Schlenk techniques. Anhydrous *n*-hexane and toluene were purchased from Sigma-Aldrich in sure-sealed reservoirs (18L) and dried by passage through activated alumina and a Q-5 columns. THF and Et_2O were distilled, under nitrogen, from sodium benzophenone ketyl and stored under sodium metal and activated 4 Å molecular sieves. Anhydrous DME was purchased from Sigma-Aldrich and passed through a column of activated alumina and stored over 4 Å molecular sieves prior to use. C_6D_6 was purchased from Cambridge Isotope Laboratory (CIL), degassed by three freeze-pump-thaw cycles and stored over 4 Å molecular sieves. Celite, alumina, and 4 Å molecular sieves were dried under vacuum overnight at 150 ºC. All other reagents were obtained from commercial sources and used as received. The nindigo ligand, $H_2dmp_2nindigo$,[1] and $Co[N(SiMe_3)_2]_2$[2] were synthesised as published. NMR spectra were recorded on a Varian Inova 400 MHz spectrometer. ^1H NMR spectra are referenced to $SiMe_4$ using the residual ^1H solvent peaks as internal standards. Elemental analyses were performed at Midwest Microlab, LLC. UV-vis/NIR spectra were recorded on a Varian Cary 5000 spectrophotometer.

Cyclic Voltammetry. Cyclic voltammetric measurements were performed using an E2 Epsilon potentiostat with a PC unit controlled by Bioanalytical systems (BAS) software. Experiments were performed under inert atmosphere using platinum working and counter electrodes with a Ag/AgCl pseudo-reference electrode. Solutions contained approximately 0.1 mM (variability in concentrations resulting from low sample mass (2-3mg) error) in metal complex with $[Bu_4N][PF_6]$ (0.1M, THF) as supporting electrolyte. All potentials are reported versus $[Cp_2Fe]^{0/+}$, referenced as internal standard.

This journal is © The Royal Society of Chemistry 2012

As calculated by the cyclic voltammetric data, the comproportionation constant $K_c = 2 \times 10^9$ ($\Delta E_{1/2}$ = 550 mV for **1**) is large, indicative of significant charge delocalization in the mixed valent state.[3] Moreover, the open circuit potential shifts towards lower values across **1** (–1.4 V), $\mathbf{[1]}^-$ (–2.0 V), and $\mathbf{[1]}^{2-}$ (–2.2 V) in accord with the decreased oxidation state of the complexes.

X-ray Crystallography. Data for $\mathbf{[1]}^-$ and $\mathbf{[1]}^{2-}$ were collected on a Bruker KAPPA APEX II Duo diffractometer equipped with an APEX II CCD detector. The data collection was carried out using Mo Kα radiation (graphite monochromator). A randomly oriented region of reciprocal space was surveyed to achieve complete data with a redundancy of 4. Sections of frames were collected with 0.50º steps in ω and ϕ scans. Crystals were mounted on a Mitigen Kapton loop, coated in NVH oil and maintained at 150(2)K under a flow of nitrogen gas during data collection. Data for **1** was collected at 100(2)K at the Advanced Photon Source in Argonne National Laboratory using synchrotron radiation (λ = 0.41328, silicon 111 and 311 monochromators, two mirrors to exclude higher harmonics). Data collection and cell parameter determination were conducted using the SMART program.[4] Integration of the data and final cell parameter refinements were performed using SAINT[5] software with data absorption correction implemented through SADABS.[6] The structures were solved using SIR-92[7] and refinement was performed using the Oxford University Crystals for Windows system.[8]

SQUID Magnetic Measurements. Magnetic susceptibility measurements were performed using a Quantum Design SQUID magnetometer MPMS-XL7 housed at the University of Ottawa operating between 1.9 and 300 K for applied dc fields ranging from -7 to 7 T. Dc analyses was performed on freshly prepared polycrystalline samples wrapped in a polyethylenemembrane (prepared in an inert atmosphere). The magnetization data was collected at 100 K to check for

ferromagnetic impurities that were absent in the sample. Diamagnetic corrections were applied for the sample holder and the core diamagnetism from the sample (estimated with Pascal constants).

Synthesis of $dmp_2Nin[Co(NR_2)]_2$ (R = $SiMe_3$) (1). To a stirring, green solution of $Co(NR_2)_2$ (0.900 g, 2.37 mmol) in toluene (15 mL) was added H_2dmp_2nindigo (0.529 g, 1.13 mmol) as a solid. Upon addition, the solution turned deep green in colour, becoming dark brown after 2 h, concomitant with the precipitation of a dark brown solid. Volatiles were removed in vacuo and the remaining solid was stirred in hexane (10 mL) forming a suspension. The suspension was filtered over a medium porosity glass frit and the collected solid was washed with hexane (3 × 10 mL) and subsequently dried under vacuum to give **1** as a dark brown solid. 0.771 g, 75% yield. Crystals of **1** were grown from a dilute solution of toluene (1 mL) and hexane (5 mL) stored at -27 °C for 2 weeks. ^{1}H NMR (400 MHz, 25 °C, C_6D_6): δ -26.93 (s, 2H), -23.03 (s, 2H), -8.91 (br s, 2H), 8.57 (s, 12H, *Me N*-aryl), 13.24 (s, 36H, NSi*Me*$_3$), 22.63 (s, 4H, meta-*CH N*-aryl), 34.29 (s, 2H, para-*CH N*-aryl), 80.92 (s, 2H). ^{1}H NMR (400 MHz, 25 °C, THF-d_8): δ -33.05 (br s, 2H), -29.37 (s, 2H), -23.36 (s, 2H), 10.67 (s, 36H, NSi*Me*$_3$), 17.60 (s, 4H, meta-*CH N*-aryl), 18.29 (s, 12H, *Me N*-aryl), 24.33 (s, 2H, para-*CH N*-aryl), 50.59 (s, 2H). μ_{eff} = 6.37(8) μ_B (C_6D_6, 298K, Evans' method). μ_{eff} = 6.02 μ_B (THF-d_8, 25 °C, Evans' method). UV-vis/NIR (toluene, 0.14 mM, 25 °C, L•mol^{-1}•cm^{-1}): 315 (ε = 32362), 446 (ε = 7993), 764 (ε = 16997). Anal. Calcd for $C_{44}H_{62}Co_2N_6Si_4$: C, 58.38; H, 6.90; N, 9.28. Found: C, 58.29; H, 6.87; N, 9.25.

Synthesis of $[K(DME)_4][dmp_2Nin\{Co(NR_2)\}_2]$ ([1]$^-$). Method A. To a stirring solution of **1** (0.402 g, 0.444 mmol) in a mixture of toluene (10 mL) and Et_2O (2 mL) was added potassium metal (0.017 g, 0.435 mmol) and anthracene (2 mg). The solution was stirred for 24 h, turning dark red and producing a deep purple precipitate. The solution was filtered over a medium

porosity frit and the collected solid was washed with hexane (3 × 5 mL). The solid was subsequently dissolved in DME (10 mL) and filtered through Celite supported on glass wool. The filtrate was concentrated to 2 mL in volume and layered with hexane (10 mL). Storage of the solution at -27 °C for 5 d produced dark purple crystals of **[1]**$^{-}$. 0.232 g, 40% yield. ^{1}H NMR (400 MHz, 22 °C, THF-d_8): δ -61.23 (s, 2H), -43.54 (s, 2H), -41.05 (br s, 2H), 3.12 (s, 4H, meta-*CH N*-aryl), 3.26 (s, 24H, DME), 3.42 (s, 16H, DME), 5.54 (s, 36H, NSi*Me*$_3$), 13.74 (s, 12H, *Me N*-aryl), 120.61 (s, 2H), 158.28 (s, 2H). μ_{eff} = 6.4(1) μ_B (THF-d_8, 25 °C, Evans' method). UV-vis/NIR (DME, 0.11 mM, 25 °C, L•mol^{-1}•cm^{-1}): 325 (ε = 21344), 380 (br shoulder, ε = 13093), 518 (ε = 13189), 578 (shoulder, ε = 8876), 807 (ε = 7147), 870 (ε = 6705), 1174 (ε = 3108). Anal Calcd for $C_{60}H_{102}Co_2KN_6O_8Si_4$: C, 55.23; H, 7.88; N, 6.44. Found: C, 55.22; H, 7.68; N, 6.32.

Synthesis of [K(DME)$_4$][dmp$_2$Nin{Co(NR$_2$)}$_2$] ([1]$^{-}$). Method B. To a stirring solution of **1** (0.404 g, 0.446 mmol) in Et_2O (10 mL) was added KC_8 (0.066 g, 0.488 mol). Upon addition, the solution immediately turned dark red-purple, generating a dark purple solid. The solution was filtered over a medium porosity frit and the collected solid was washed with hexane (3 × 5 mL). The solid was subsequently dissolved in DME (10 mL) and filtered through Celite supported on glass wool. The purple filtrate was concentrated to 2 mL in volume and layered with hexane (10 mL). Storage of the solution at -27 °C for 5 d produced dark purple crystals of **[1]**$^{-}$. 0.430 g, 74% yield.

Synthesis of [K(Et$_2$O)$_2$]$_2$[dmp$_2$Nin{Co(NR$_2$}$_2$] ([1]$^{2-}$). Method A. To a stirring solution of **1** (0.398 g, 0.440 mmol) in Et_2O (10 mL) was added potassium metal (0.035 g, 0.895 mmol) and anthracene (2 mg). The solution was stirred for 24 h, turning dark red. The solution was filtered through Celite supported on glass wool. The filtrate was concentrated to 3 mL in volume and stored -27 °C for 24 h, producing **[1]**$^{2-}$ as dark red crystals. Crystals of **[1]**$^{2-}$ immediately turn

opaque upon application of vacuum, owing to the consistent loss of two molecules of Et_2O as indicated by integration of the resonances in the ^1H NMR spectra. 0.214 g, 43% yield. ^1H NMR (400 MHz, 25 °C, THF-d_8): δ -58.79 (s, 2H), -9.30 (s, 2H), -2.04 (s, 36H, NSi*Me*$_3$), 1.16 (t, 12H, Et_2O), 2.45 (s, 2H), 3.43 (q, 8H, Et_2O), 30.00 (br s, 2H), 30.23 (s, 4H, meta-*CH N*-aryl), 36.14 (s, 12H, *Me N*-aryl), 51.60 (s, 2H). μ_{eff} = 6.2(2) μ_B (THF-d_8, 25 °C, Evans' method). UV-vis/NIR (Et_2O, 0.13 mM, 25 °C, L•mol^{-1}•cm^{-1}): 302 (ε = 26541), 500 (ε = 11326), 825 (ε = 2844). Anal Calcd for $[K(Et_2O)_2]_2[dmp_2Nin\{Co(NR_2\}_2]$, $C_{60}H_{102}Co_2K_2N_6O_4Si_4$: C, 56.30; H, 8.03; N, 6.57. Anal Calcd for $[K(Et_2O)]_2[dmp_2Nin\{Co(NR_2\}_2]$, $C_{52}H_{82}Co_2K_2N_6O_2Si_4$: C, 55.19; H, 7.30; N, 7.43. Found: C, 54.91; H, 7.42; N, 6.44.

Synthesis of $[K(Et_2O)_2]_2[dmp_2Nin\{Co(NR_2\}_2]$ ($[1]^{2-}$). Method B. To a stirring solution of **1** (0.403 g, 0.445 mmol) in Et_2O (10 mL) was added KC_8 (0.126 g, 0.932 mol). Upon addition, the solution immediately turned dark orange-red. The solution was filtered through Celite supported on glass wool. The filtrate was concentrated to 3 mL in volume and stored -27 °C for 24 h, producing $[1]^{2-}$ as dark red crystals. 0.456 g, 90% yield based on $[K(Et_2O)]_2[dmp_2Nin\{Co(NR_2\}_2]$.

This journal is © The Royal Society of Chemistry 2012

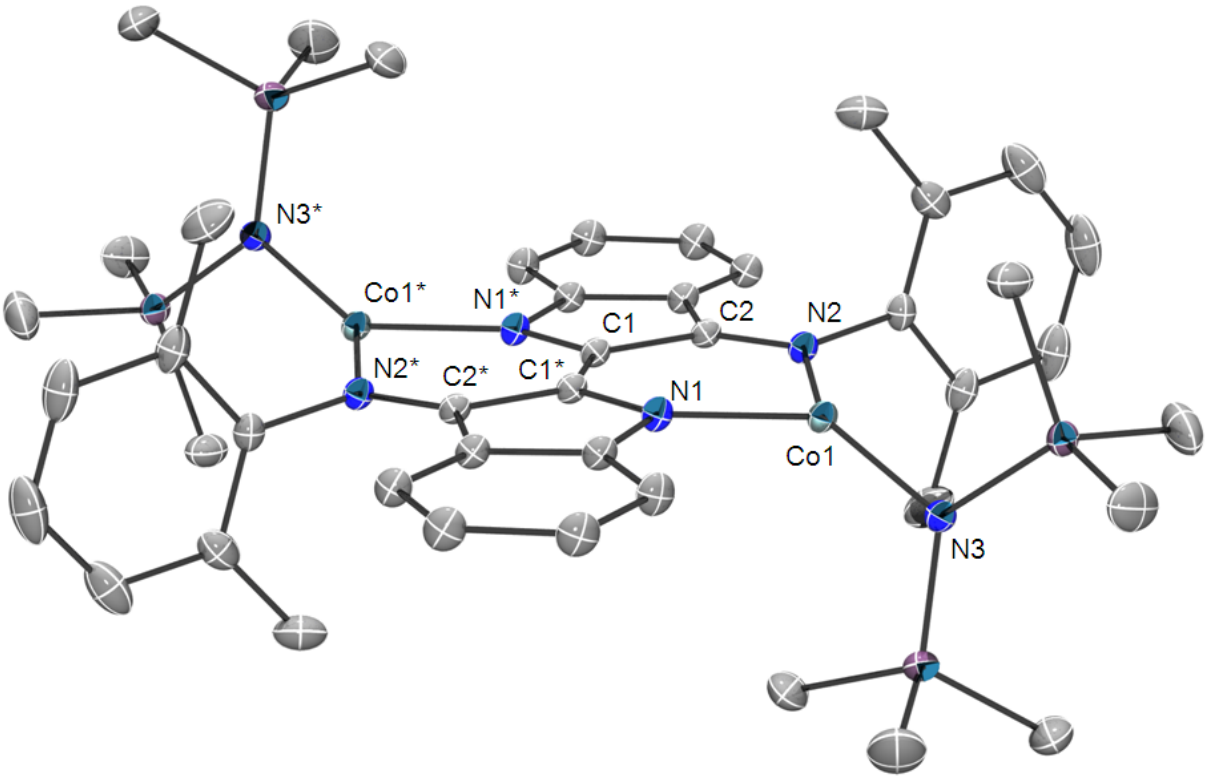

Figure S1. Solid state molecular structure of **1** with 40% probability ellipsoids. Asterisks denote symmetry generated atoms. Selected bond lengths (Å) and angles (°) for **1**: Co1-N1 = 1.9301(9), Co1-N2 = 1.9569(8), Co1-N3 = 1.8792(8), C1-C1* = 1.393(2), C2-N2 = 1.321(1), C1-C2 = 1.466(1), N1-Co1-N2 = 95.80(3), N1-Co1-N3 = 126.42(4), N2-Co1-N3 = 133.19(4).

This journal is © The Royal Society of Chemistry 2012

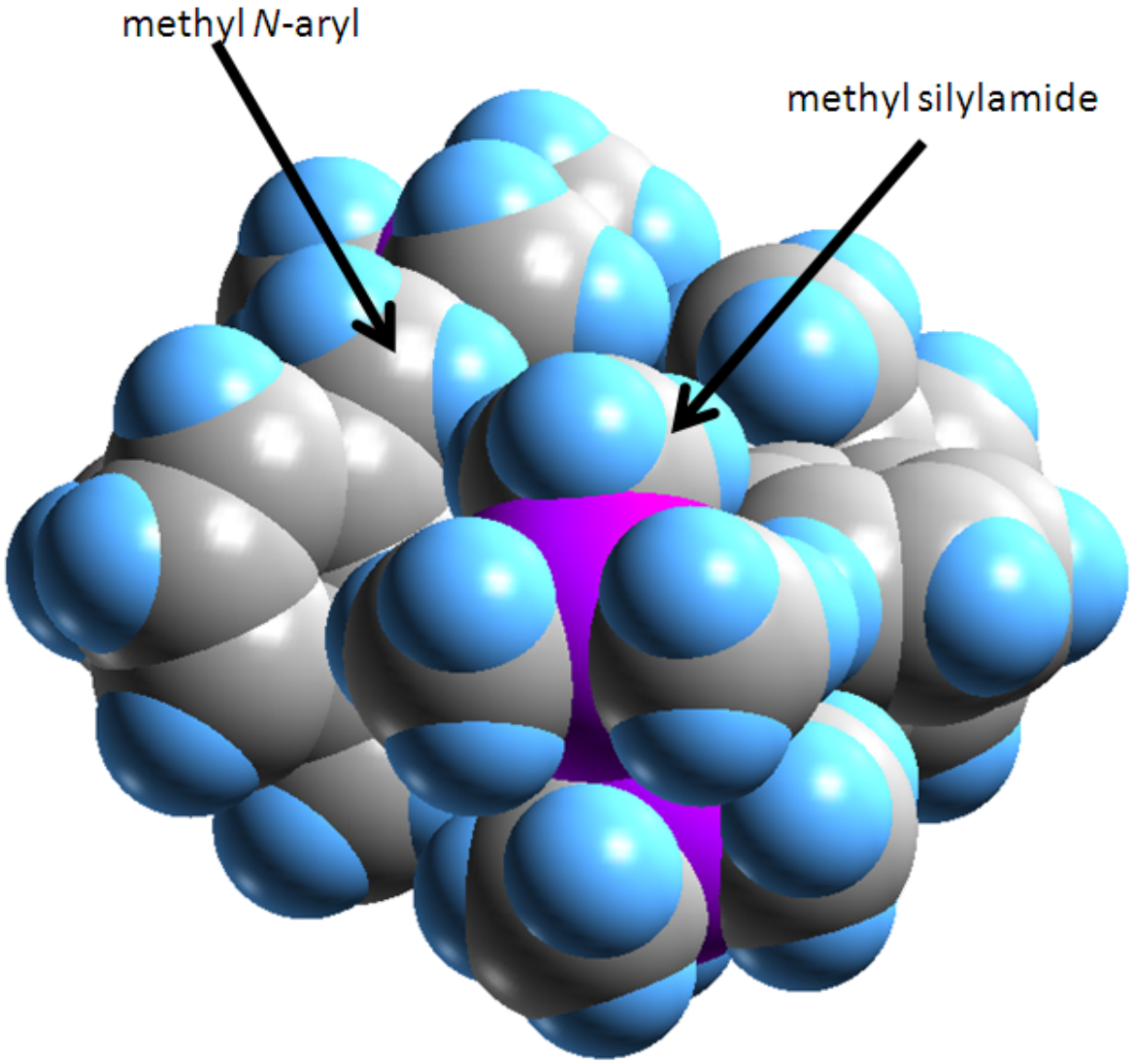

Figure S2. Space filling model of **1** along the Co-N_{amide} vector, revealing steric interaction between methyls of the *N*-aryl and silylamide substituents. Blue, grey and purple spheres represent hydrogen, carbon, and silicon atoms, respectively.

This journal is © The Royal Society of Chemistry 2012

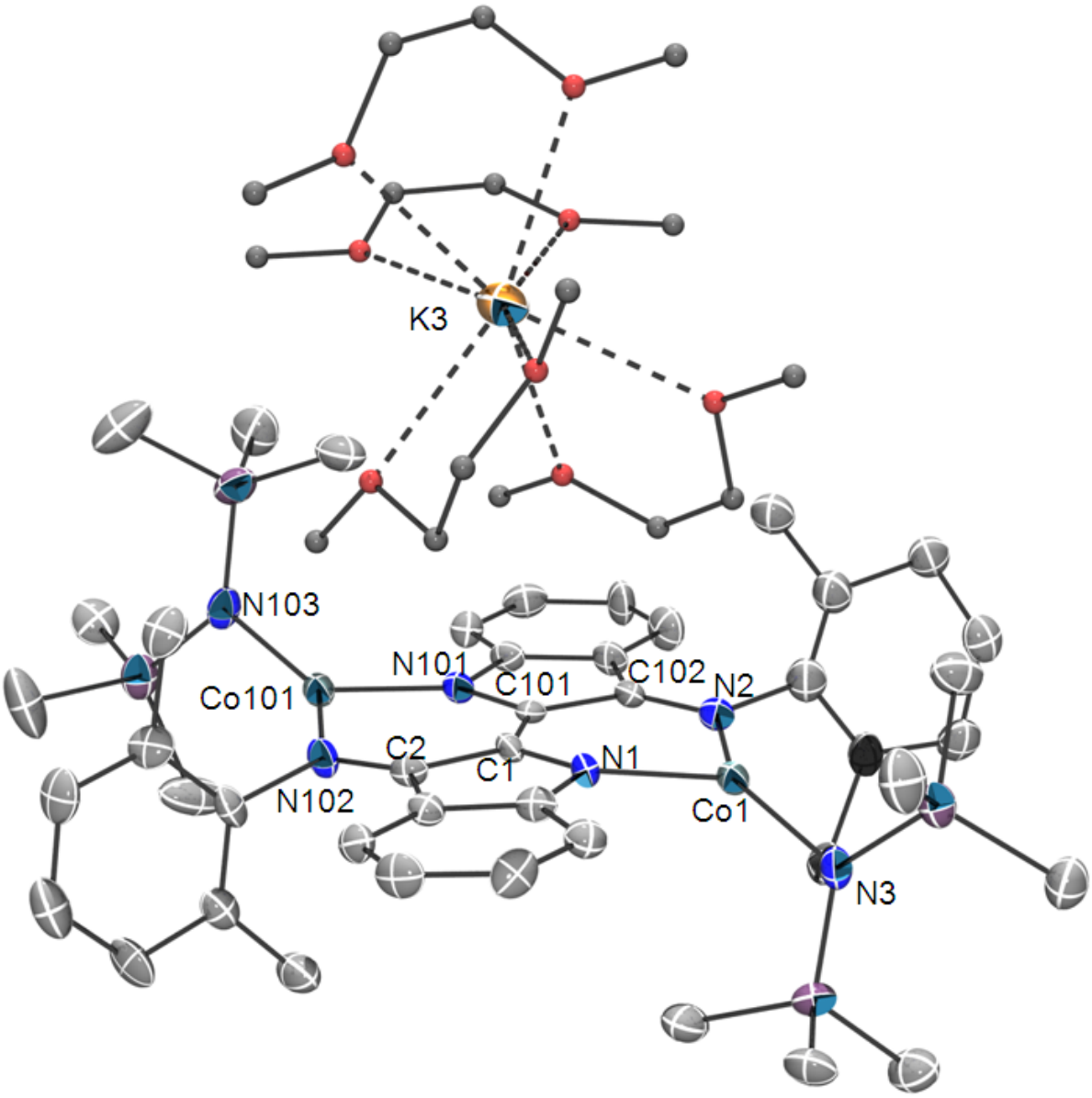

Figure S3. Solid state molecular structure of **[1]**$^-$ with 30% probability ellipsoids. Selected bond lengths (Å) and angles (°) for **[1]**$^-$: Co1-N1 = 1.969(7), Co1-N2 = 1.919(8), Co1-N3 = 1.929(8), C1-C101 = 1.40(1), C102-N2 = 1.35(1), C1-C2 = 1.46(1), N1-Co1-N2 = 95.3(3), N1-Co1-N3 = 125.3(4), N2-Co1-N3 = 136.5(4).

This journal is © The Royal Society of Chemistry 2012

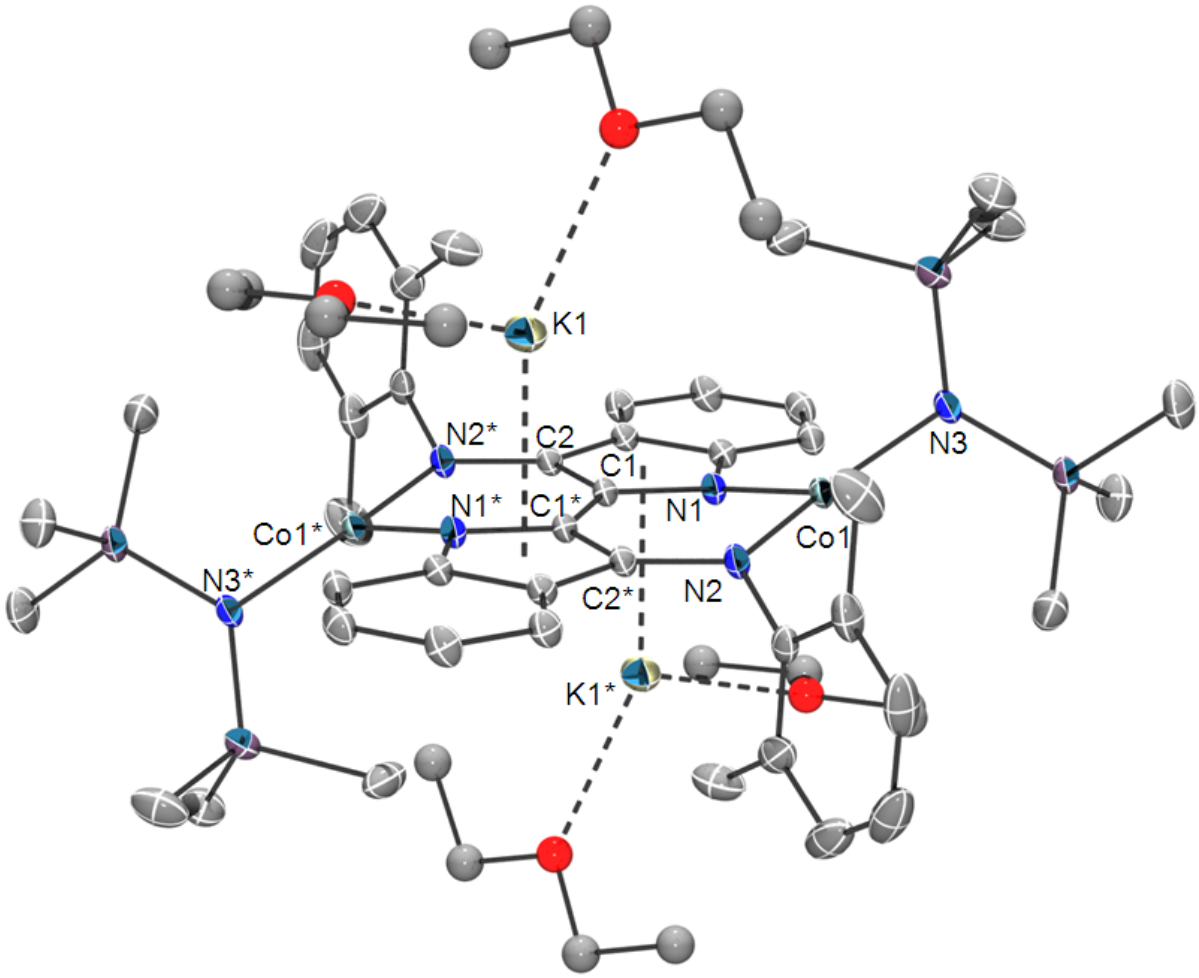

Figure S4. Solid state molecular structure of $[\mathbf{1}]^{2-}$ with 40% probability ellipsoids. Asterisks denote symmetry generated atoms. Selected bond lengths (Å) and angles (°) for $[\mathbf{1}]^{2-}$: Co1-N1 = 1.973(1), Co1-N2 = 1.901(1), Co1-N3 = 1.913(1), C1-C1* = 1.438(8), C2*-N2 = 1.401(2), C1-C2 = 1.404(2), N1-Co1-N2 = 97.87(5), N1-Co1-N3 = 120.82(5), N2-Co1-N3 = 138.52(6).

This journal is © The Royal Society of Chemistry 2012

Table S1. X-ray Crystallographic Data for **1**, $[\mathbf{1}]^-$ and $[\mathbf{1}]^{2-}$.

	1	$[\mathbf{1}]^-$	$[\mathbf{1}]^{2-}$
Empirical formula	$C_{44}H_{62}Co_2N_6Si_4$	$C_{60}H_{102}Co_2KN_6O_8Si_4$	$C_{60}H_{102}Co_2K_2N_6O_4Si_4$
Crystal Habit, colour	irregular, dark brown	prism, purple	plate, dark red
Crystal size (mm)	0.080 × 0.060 × 0.056	0.596 × 0.244 × 0.106	0.50 × 0.180 × 0.541
Crystal system	orthorhombic	orthorhombic	monoclinic
Space group	*Pbca*	*Fdd*2	$P2_1/n$
Volume ($Å^3$)	4807.6(2)	57576(12)	3467.3(6)
a (Å)	14.5775(4)	37.418(3)	13.359(1)
b (Å)	17.1584(5)	48.552(2)	12.811(1)
c (Å)	19.2207(6)	31.729(1)	20.986(2)
α(°)	90	90	90
β□□(°)	90	90	105.108(2)
γ□□(°)	90	90	90
Z	4	32	2
Formula weight (g/mol)	905.23	1304.82	1279.91
Density (calculated) (Mg/m^3)	1.251	1.203	1.226
Absorption coefficient (mm^{-1})	0.826	0.635	0.713
F_{000}	1912	22304	1368
Total no. reflections	124878	138041	73885
Unique reflections	16577	34323	10151
Final R indices ($I > 2\sigma(I)$]	$R_1 = 0.0382$, $wR_2 = 0.0901$	$R_1 = 0.0717$, $wR_2 = 0.1744$	$R_1 = 0.0324$, $wR_2 = 0.0739$
Largest diff. peak and hole ($e^-Å^{-3}$)	0.96 and -1.25	2.234 and -0.436	0.58 and -0.74
GOF	0.9547	1.357	0.9910

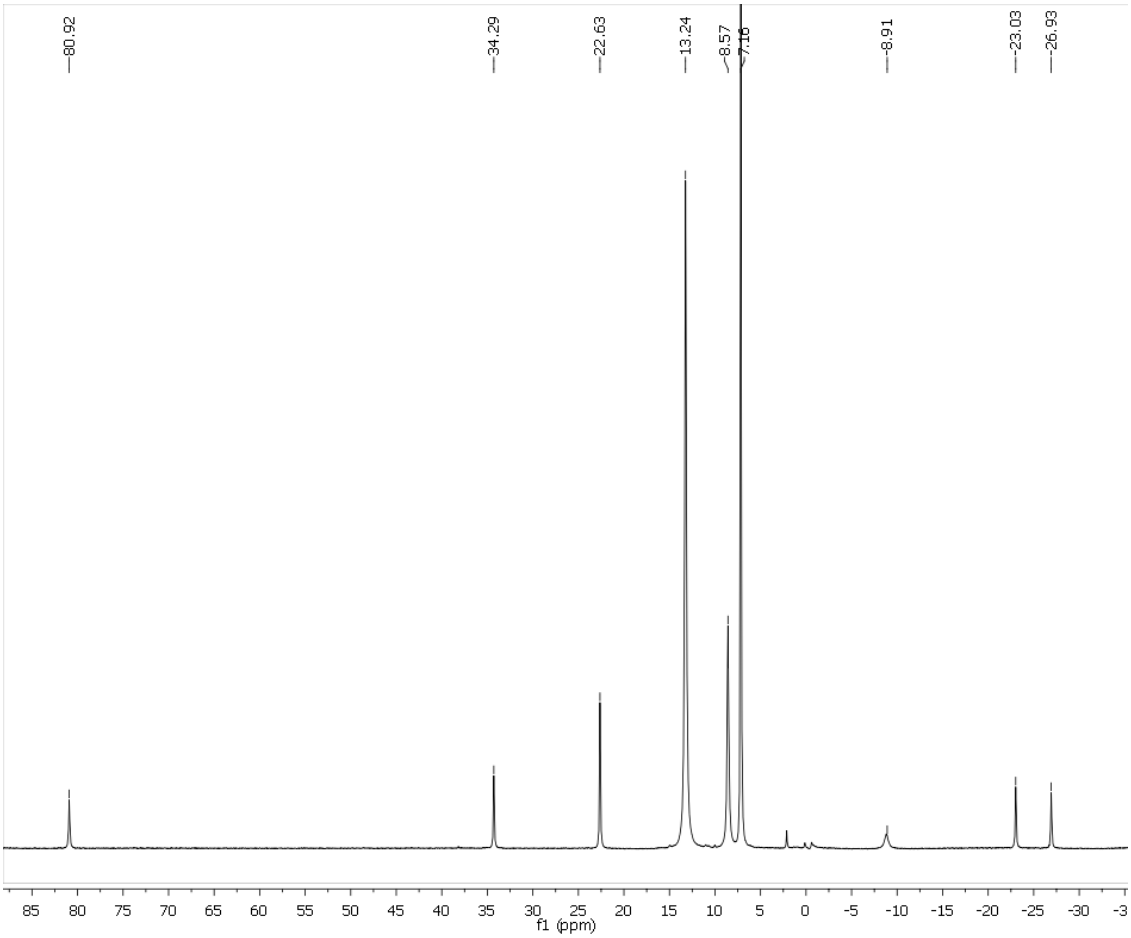

Figure S5. ^{1}H NMR spectrum of **1** in C_6D_6.

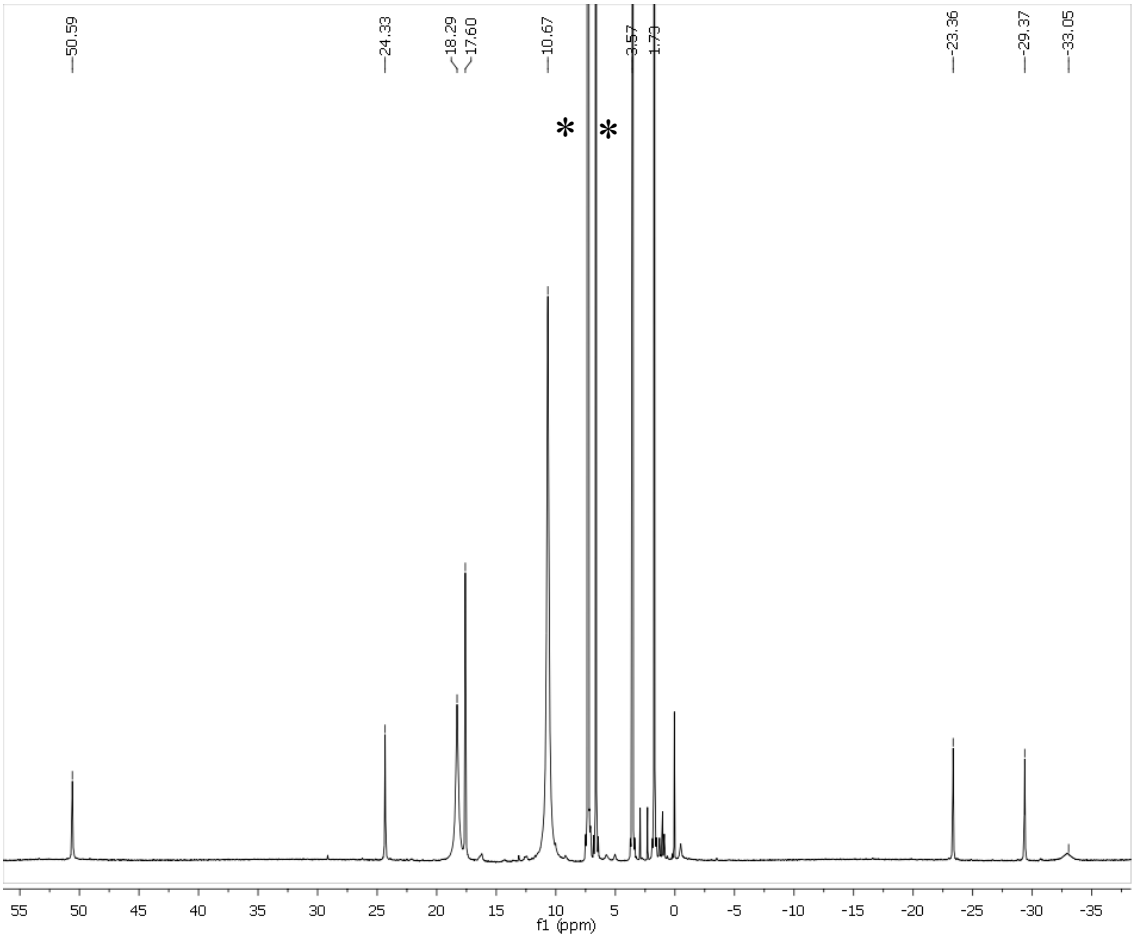

Figure S6. ^{1}H NMR spectrum of **1** in THF-d_8. Asterisks denote C_6H_6 resonances utilized for Evans' measurement.

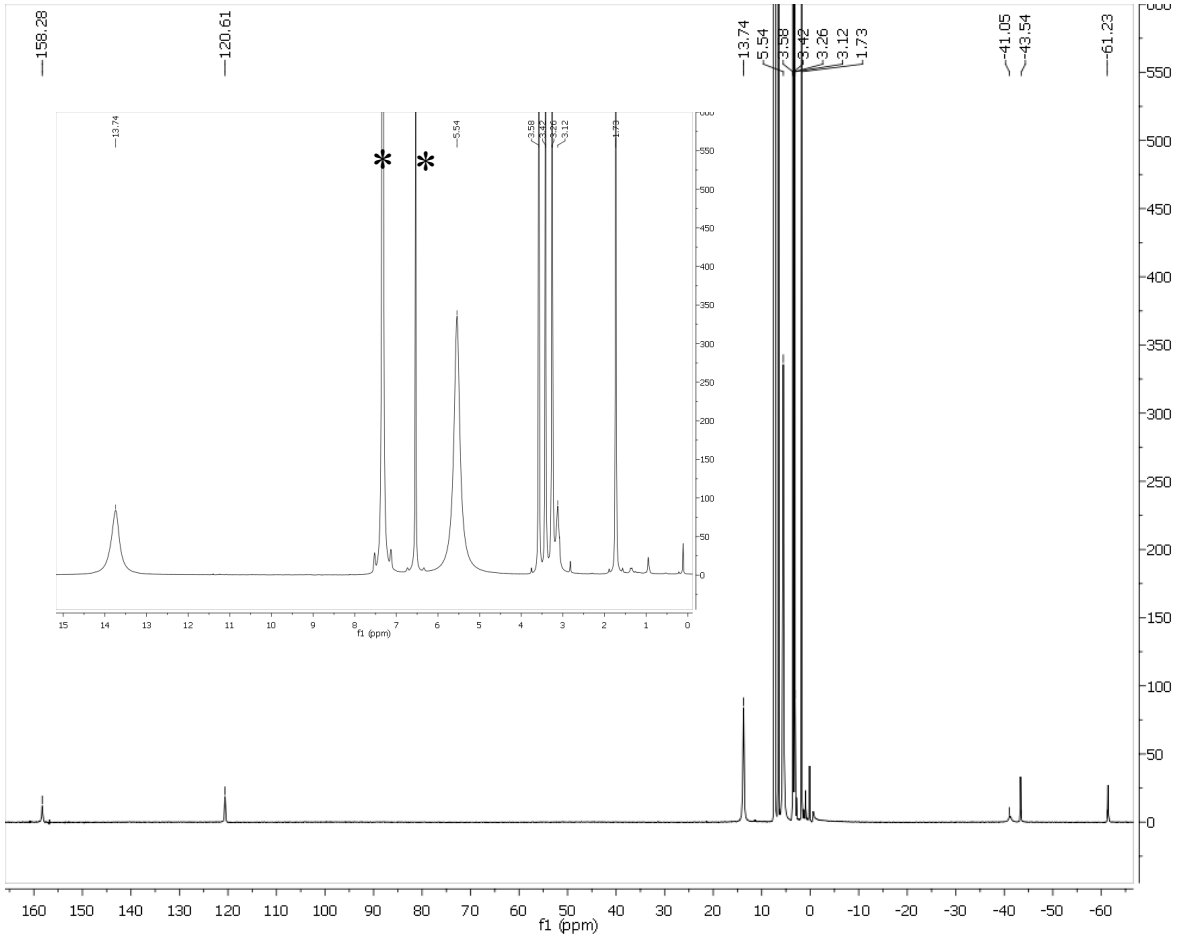

Figure S7. ^{1}H NMR spectrum of **[1]**$^{-}$ in THF-d_8. Asterisks denote C_6H_6 resonances utilized for Evans' measurement.

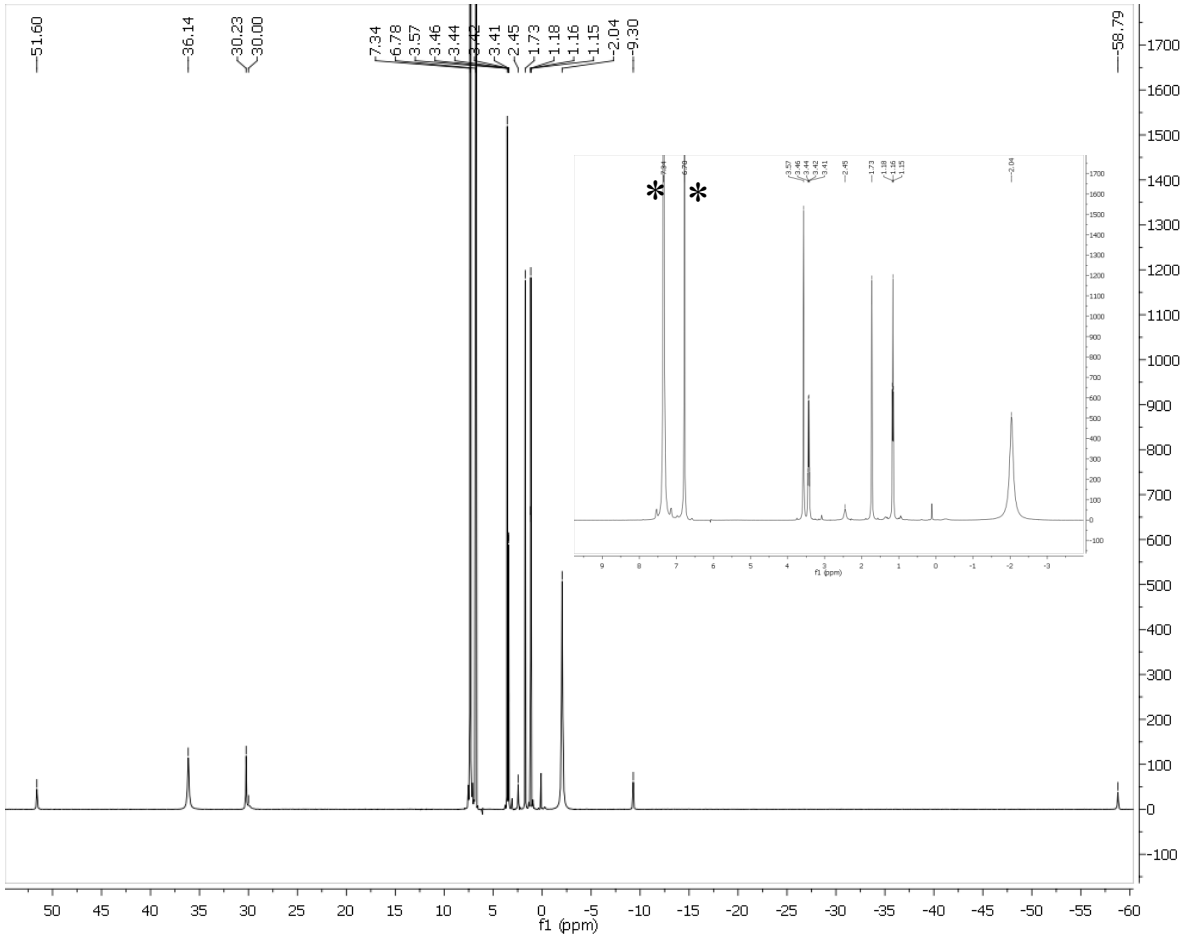

Figure S8. ^{1}H NMR spectrum of **[1]$^{2-}$** in THF-d_8. Asterisks denote C_6H_6 resonances utilized for Evans' measurement.

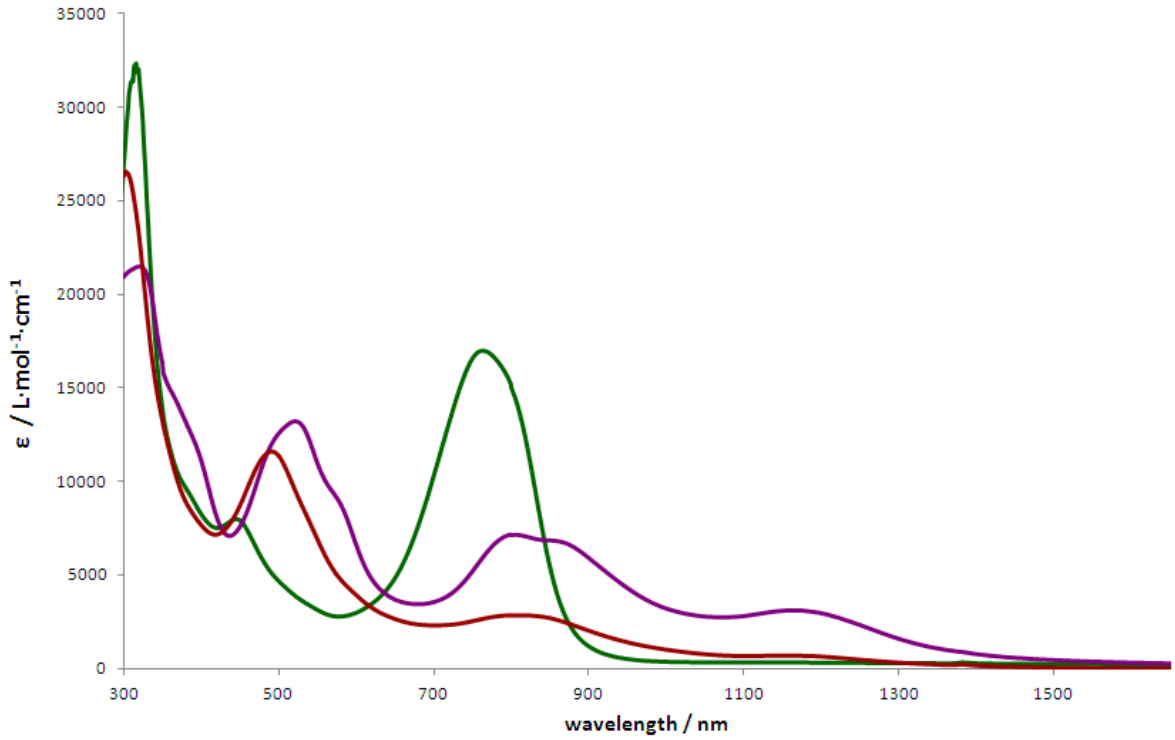

Figure S9. Room temperature UV-vis/NIR absorption spectra for **1** (toluene, 0.14 mM), **[1]**$^{-}$ (DME, 0.11 mM) and **[1]**$^{2-}$ (Et_2O, 0.13 mM).

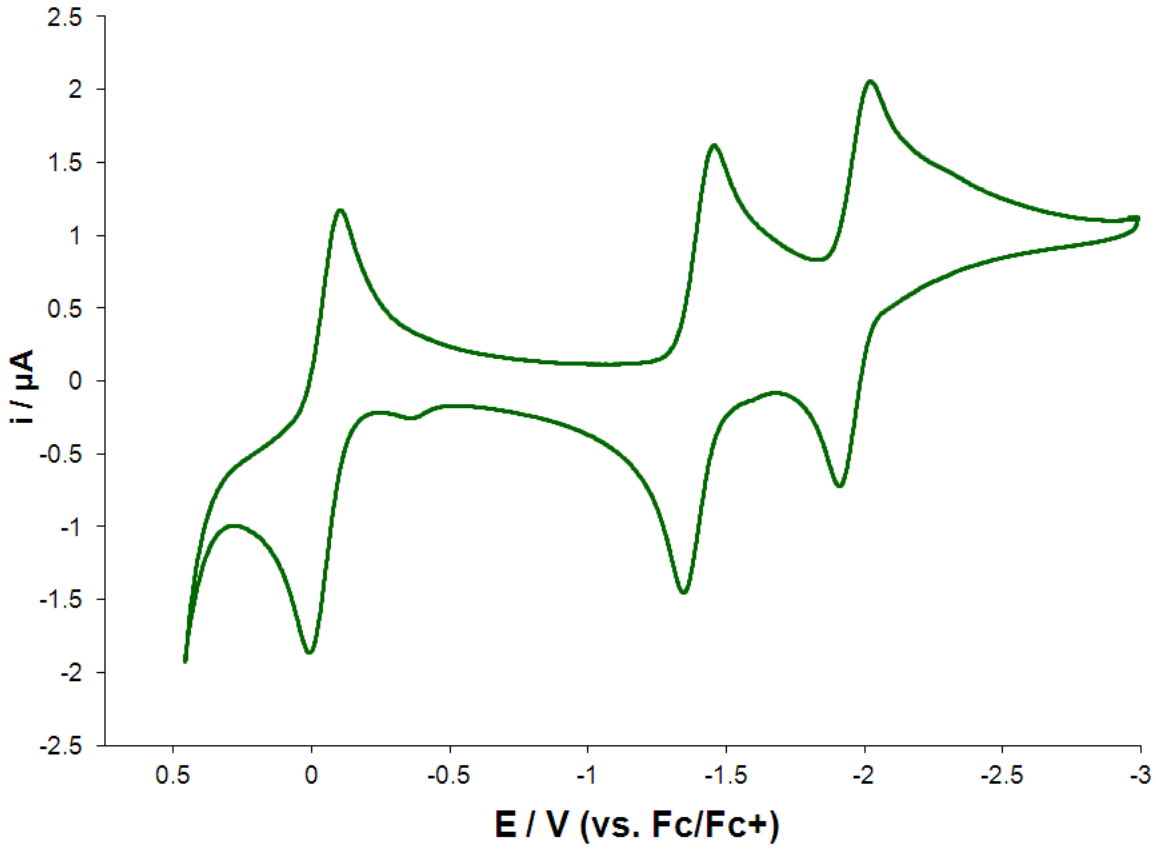

Figure S10. Room temperature cyclic voltammogram of **1** in THF vs $[Cp_2Fe]^{0/+}$. (Scan rate 200 mv/s; 0.1 M $[NBu_4][PF_6]$ as supporting electrolyte.)

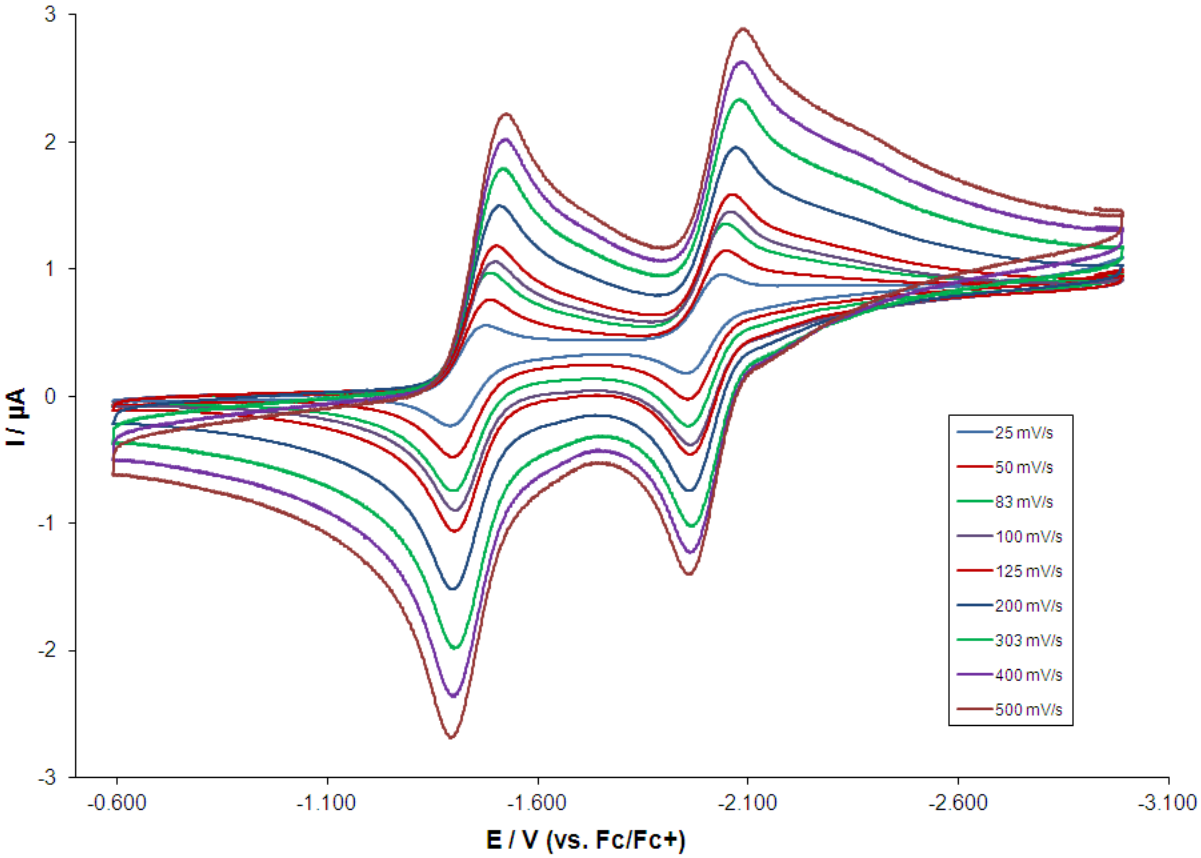

Figure S11. Room temperature cyclic voltammogram of **1** in THF vs $[Cp_2Fe]^{0/+}$.

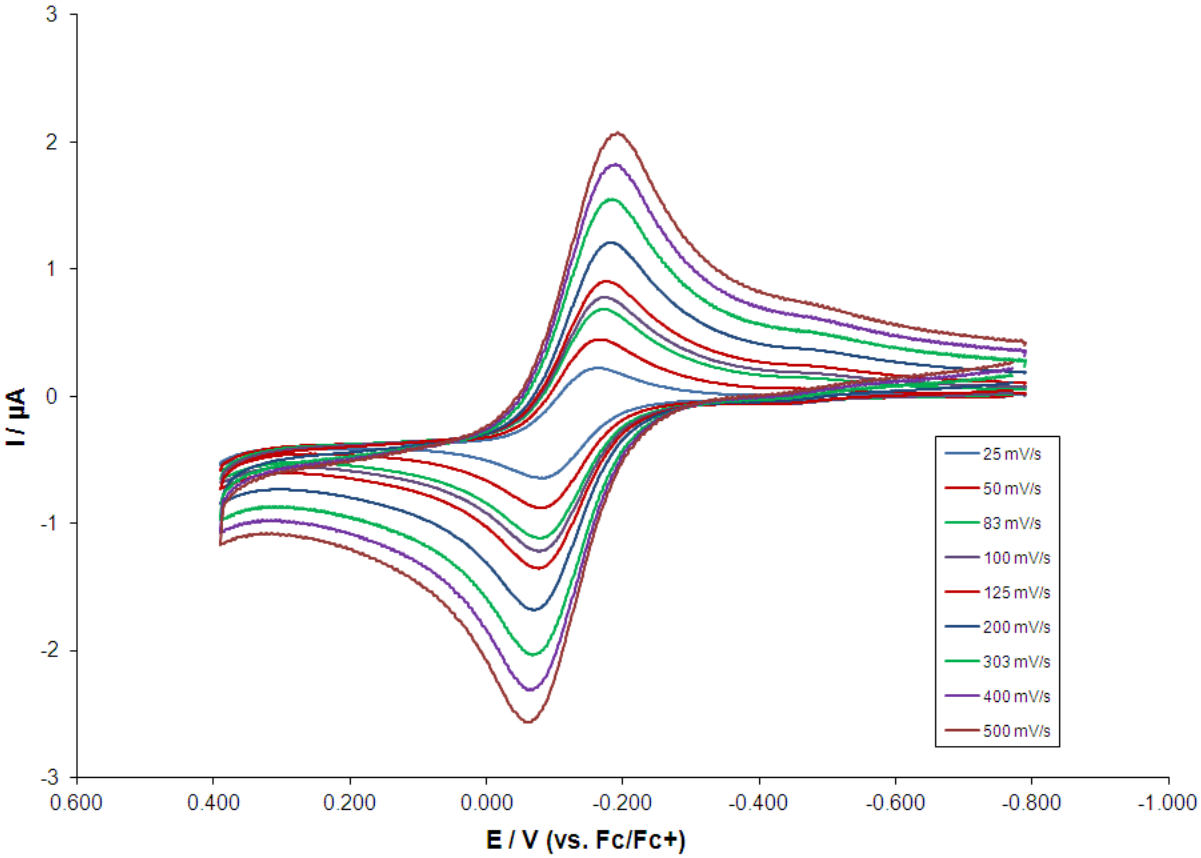

Figure S12. Room temperature cyclic voltammogram of **1** in THF vs $[Cp_2Fe]^{0/+}$.

This journal is © The Royal Society of Chemistry 2012

Table S2. Electrochemical data for **1** in THF (vs. $[Cp_2Fe]^{0/+}$).

Reduction feature 1	**Scan rate, V/s**	$E_{p,c}$, V	$E_{p,a}$, V	ΔE_p, V	$i_{p,c}/i_{p,a}$
	0.025	-1.474	-1.393	0.081	0.88
	0.050	-1.484	-1.401	0.083	0.96
	0.083	-1.484	-1.398	0.086	1.00
	0.100	-1.498	-1.402	0.096	1.02
	0.125	-1.502	-1.402	0.1	0.93
	0.200	-1.509	-1.399	0.11	0.93
	0.303	-1.518	-1.401	0.117	1.07
	0.400	-1.521	-1.402	0.119	1.05
	0.500	-1.525	-1.392	0.133	1.05
Reduction feature 2	**Scan rate, V/s**	$E_{p,c}$, V	$E_{p,a}$, V	ΔE_p, V	$i_{p,c}/i_{p,a}$
	0.025	-2.03	-1.953	0.077	1.18
	0.050	-1.76	-1.957	-0.197	1.05
	0.083	-2.047	-1.959	0.088	1.07
	0.100	-2.06	-1.964	0.096	0.96
	0.125	-2.063	-1.964	0.099	0.96
	0.200	-2.069	-1.959	0.11	0.91
	0.303	-2.078	-1.966	0.112	0.87
	0.400	-2.087	-1.961	0.126	0.89
	0.500	-2.091	-1.958	0.133	0.85
Oxidation Feature	**Scan rate, V/s**	$E_{p,c}$, V	$E_{p,a}$, V	ΔE_p, V	$i_{p,c}/i_{p,a}$
	0.025	-0.165	-0.079	0.086	1.21
	0.050	-0.166	-0.083	0.083	1.01
	0.083	-0.173	-0.077	0.096	0.91
	0.100	-0.172	-0.077	0.095	0.93
	0.125	-0.174	-0.077	0.097	0.95
	0.200	-0.18	-0.069	0.111	0.99
	0.303	-0.185	-0.068	0.117	1.05
	0.400	-0.189	-0.062	0.127	0.90
	0.500	-0.193	-0.058	0.135	0.92

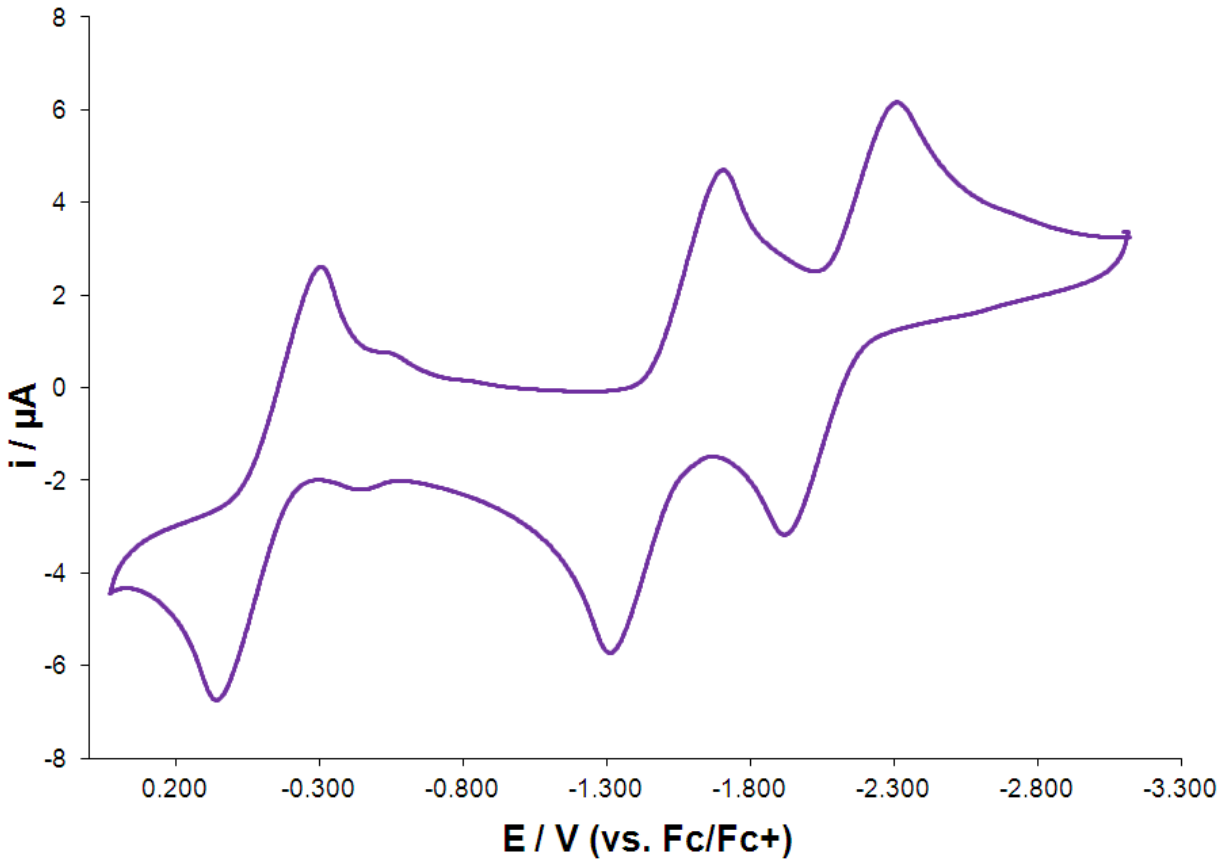

Figure S13. Room temperature cyclic voltammogram of **[1]**$^{-}$ in THF vs $[Cp_2Fe]^{0/+}$. (Scan rate 200 mv/s; 0.1 M $[NBu_4][PF_6]$ as supporting electrolyte.)

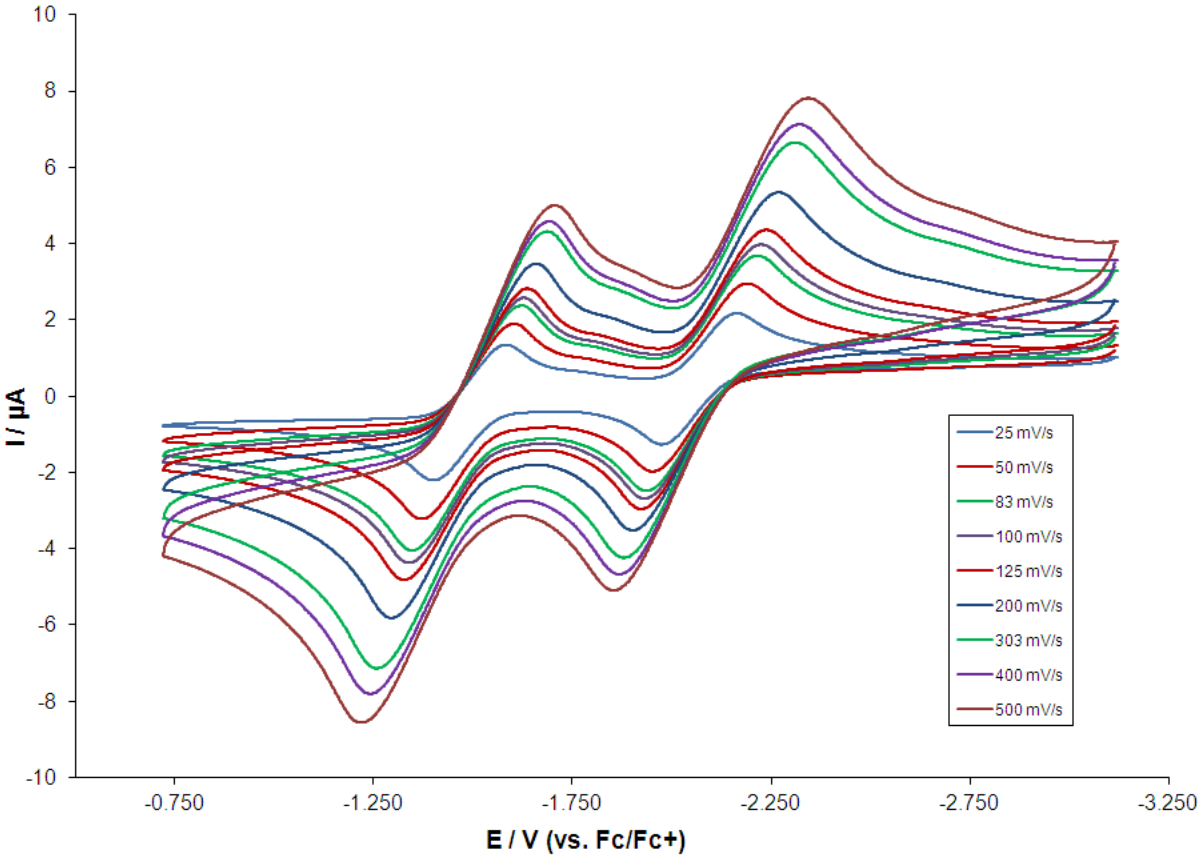

Figure S14. Room temperature cyclic voltammogram of **[1]**$^{-}$ in THF vs $[Cp_2Fe]^{0/+}$.

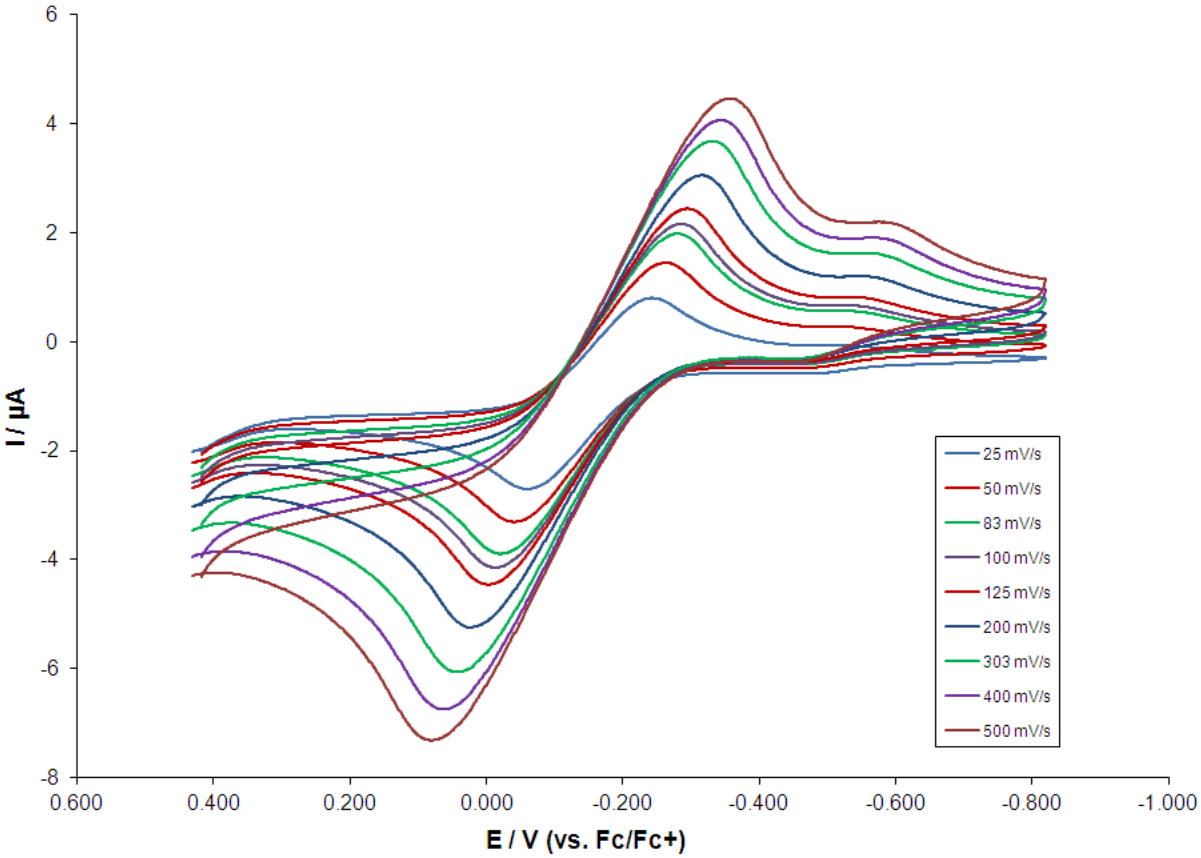

Figure S15. Room temperature cyclic voltammogram of **[1]**$^{-}$ in THF vs $[Cp_2Fe]^{0/+}$.

This journal is © The Royal Society of Chemistry 2012

Table S3. Electrochemical data for **[1]**$^-$ in THF (vs. $[Cp_2Fe]^{0/+}$).

Reduction feature	**Scan rate, V/s**	**$E_{p,c}$, V**	**$E_{p,a}$, V**	**ΔE_p, V**	**$i_{p,c}/i_{p,a}$**
	0.025	-2.164	-1.976	0.188	0.94
	0.050	-2.189	-1.951	0.238	0.88
	0.083	-2.216	-1.938	0.278	0.96
	0.100	-2.224	-1.933	0.291	0.94
	0.125	-2.238	-1.922	0.316	0.94
	0.200	-2.269	-1.902	0.367	0.97
	0.303	-2.312	-1.882	0.43	1.02
	0.400	-2.323	-1.868	0.455	0.94
	0.500	-2.343	-1.857	0.486	1.02
Oxidation Feature 1	**Scan rate, V/s**	**$E_{p,c}$, V**	**$E_{p,a}$, V**	**ΔE_p, V**	**$i_{p,c}/i_{p,a}$**
	0.025	-1.582	-1.403	0.179	1.06
	0.050	-1.601	-1.372	0.229	1.08
	0.083	-1.625	-1.348	0.277	1.10
	0.100	-1.627	-1.338	0.289	1.10
	0.125	-1.636	-1.327	0.309	1.06
	0.200	-1.658	-1.296	0.362	1.05
	0.303	-1.688	-1.26	0.428	1.00
	0.400	-1.69	-1.242	0.448	0.94
	0.500	-1.703	-1.217	0.486	0.93
Oxidation Feature 2	**Scan rate, V/s**	**$E_{p,c}$, V**	**$E_{p,a}$, V**	**ΔE_p, V**	**$i_{p,c}/i_{p,a}$**
	0.025	-0.243	-0.06	0.183	0.89
	0.050	-0.264	-0.041	0.223	1.04
	0.083	-0.278	-0.02	0.258	0.97
	0.100	-0.284	-0.013	0.271	0.89
	0.125	-0.295	-0.003	0.292	0.90
	0.200	-0.317	0.024	0.341	0.90
	0.303	-0.329	0.045	0.374	0.88
	0.400	-0.341	0.064	0.405	0.78
	0.500	-0.358	0.081	0.439	0.81

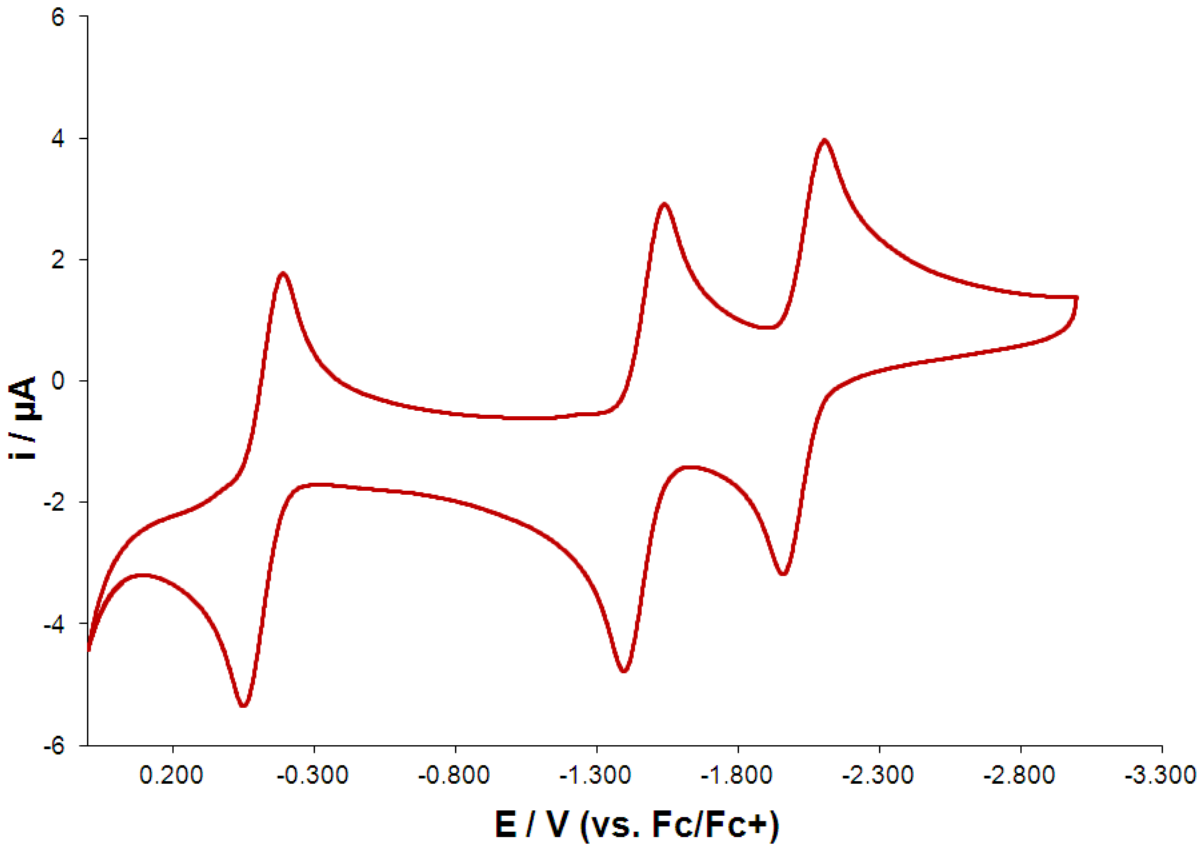

Figure S16. Room temperature cyclic voltammogram of **[1]**$^{2-}$ in THF vs $[Cp_2Fe]^{0/+}$. (Scan rate 200 mv/s; 0.1 M $[NBu_4][PF_6]$ as supporting electrolyte.)

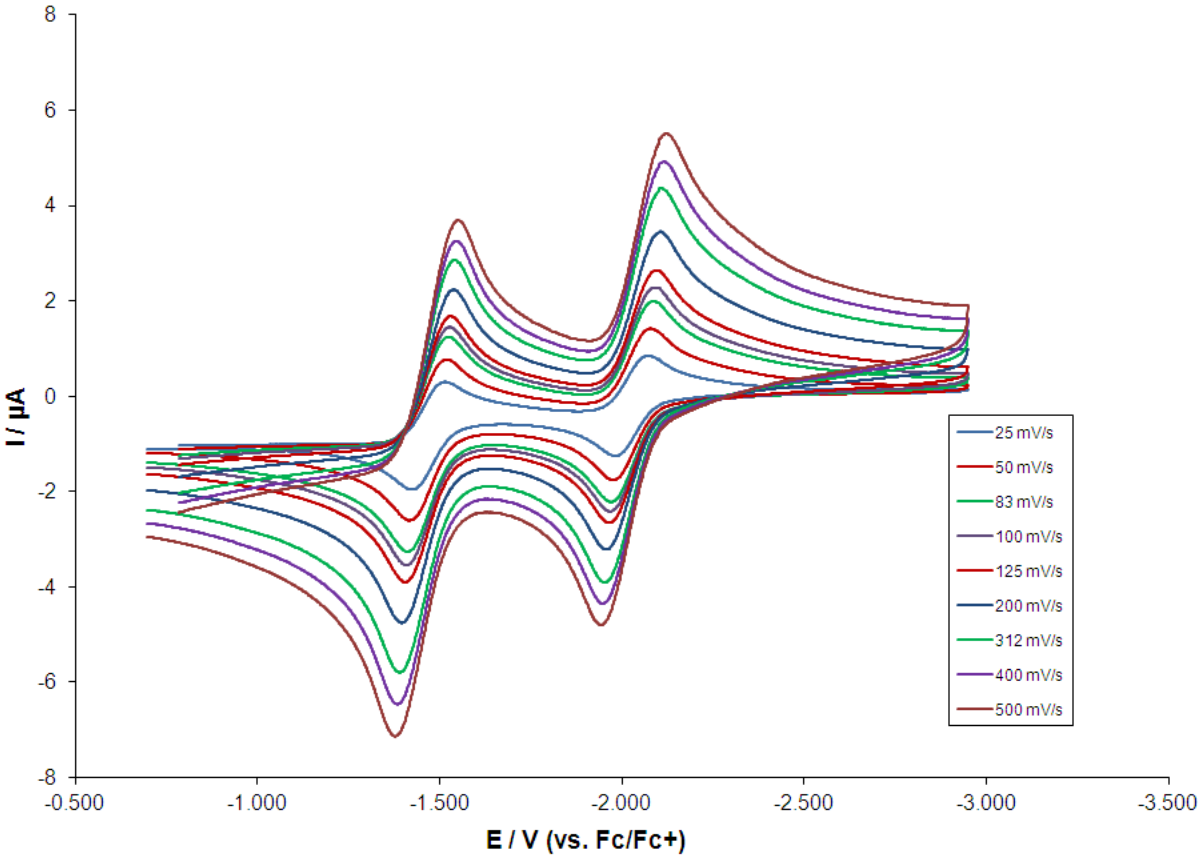

Figure S17. Room temperature cyclic voltammogram of **[1]**$^{2-}$ in THF vs $[Cp_2Fe]^{0/+}$.

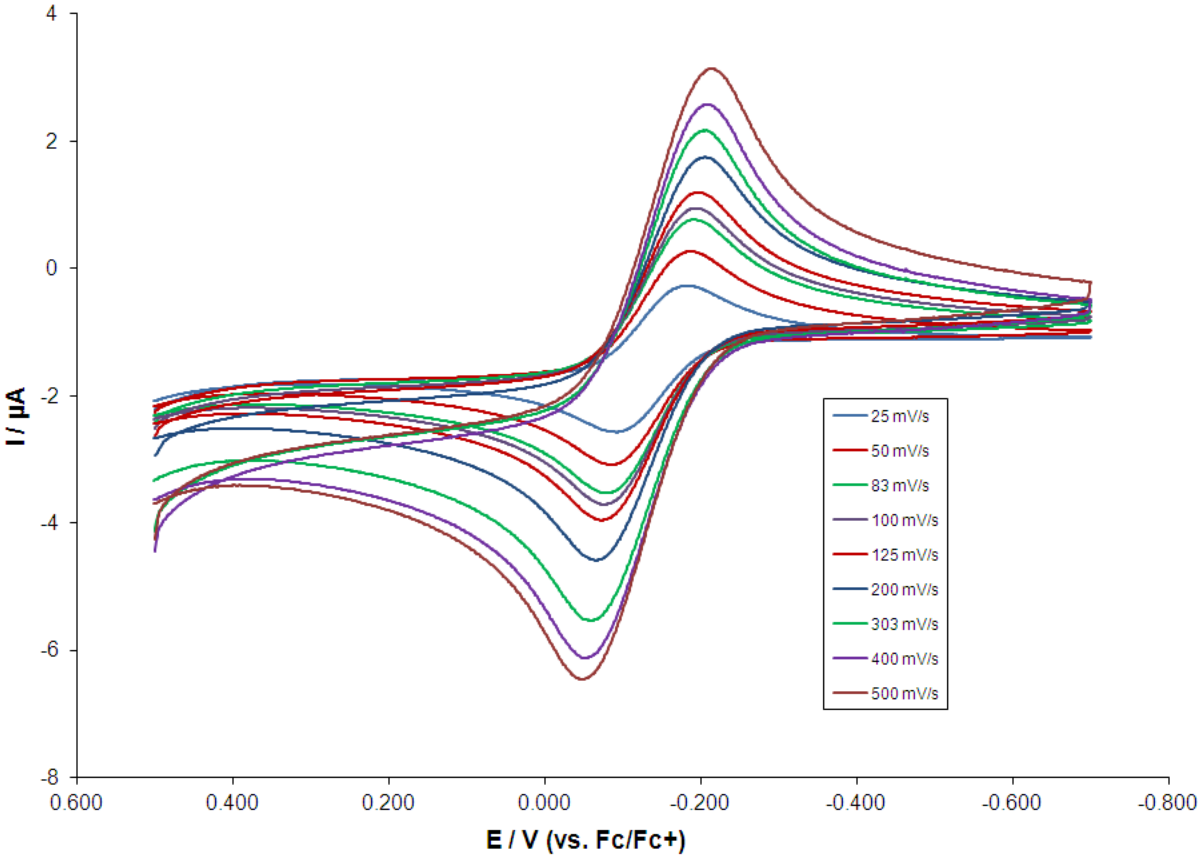

Figure S18. Room temperature cyclic voltammogram of $\mathbf{[1]^{2-}}$ in THF vs $[Cp_2Fe]^{0/+}$.

This journal is © The Royal Society of Chemistry 2012

Table S4. Electrochemical data for $[\mathbf{1}]^{2-}$ in THF (vs. $[Cp_2Fe]^{0/+}$).

Oxidation feature 1	**Scan rate, V/s**	$\mathbf{E_{p,c}}$**, V**	$\mathbf{E_{p,a}}$**, V**	$\mathbf{\Delta E_{p,a}}$**, V**	$\boldsymbol{i_{p,c}/i_{p,a}}$
	0.025	-2.072	-1.985	-0.087	1.00
	0.050	-2.078	-1.978	-0.1	1.11
	0.083	-2.085	-1.97	-0.115	1.05
	0.100	-2.087	-1.968	-0.119	0.95
	0.125	-2.094	-1.965	-0.129	0.92
	0.200	-2.106	-1.958	-0.148	0.90
	0.303	-2.106	-1.954	-0.152	0.89
	0.400	-2.113	-1.945	-0.168	0.88
	0.500	-2.119	-1.942	-0.177	1.07
Oxidation feature 2	**Scan rate, V/s**	$\mathbf{E_{p,c}}$**, V**	$\mathbf{E_{p,a}}$**, V**	$\mathbf{\Delta E_{p,a}}$**, V**	$\boldsymbol{i_{p,c}/i_{p,a}}$
	0.025	-1.516	-1.425	0.091	0.92
	0.050	-1.517	-1.417	0.1	0.98
	0.083	-1.524	-1.411	0.113	0.95
	0.100	-1.524	-1.408	0.116	1.00
	0.125	-1.53	-1.405	0.125	1.00
	0.200	-1.538	-1.396	0.142	1.03
	0.303	-1.54	-1.39	0.15	1.05
	0.400	-1.543	-1.383	0.16	1.02
	0.500	-1.549	-1.377	0.172	0.94
Oxidation feature 3	**Scan rate, V/s**	$\mathbf{E_{p,c}}$**, V**	$\mathbf{E_{p,a}}$**, V**	$\mathbf{\Delta E_{p,a}}$**, V**	$\boldsymbol{i_{p,c}/i_{p,a}}$
	0.025	-0.181	-0.091	0.09	0.93
	0.050	-0.186	-0.084	0.102	0.98
	0.083	-0.192	-0.077	0.115	0.96
	0.100	-0.193	-0.075	0.118	0.93
	0.125	-0.196	-0.073	0.123	1.04
	0.200	-0.205	-0.066	0.139	0.97
	0.303	-0.203	-0.059	0.144	0.98
	0.400	-0.21	-0.05	0.16	1.02
	0.500	-0.212	-0.048	0.164	1.02

This journal is © The Royal Society of Chemistry 2012

References

1 S. R. Oakley, G. Nawn, K. M. Waldie, T. D. MacInnis, B. O. Patrick and R. G. Hicks, *Chem. Commun.*, 2010, 46, 6753.

2 H. Burger and U. Wannagat, *Monatsh. Chem.*, 1963, 94, 1007.

3 D. M. D'Alessandro and F. R. Keene, *Chem Soc Rev*, 2006, 35; W. L. Man, G. Chen, S. M. Yiu, L. Shek, W. Y. Wong, W. T. Wong and T. C. Lau, *Dalton Trans.*, 2010, 39.

4 Bruker AXS Inc., Madison, WI, Version 2.1 edn., 2005.

5 Bruker AXS Inc., Madison, WI, Version 7.34a edn., 2005.

6 R. Blessing, *Acta Crystallogr. Sect. A: Found. Crystallogr.*, 1995, A51, 33.

7 A. Altomare, G. Cascarano, G. Giacovazzo, A. Guagliardi, M. C. Burla, G. Polidori and M. Camalli, *J. Appl. Crystallogr.*, 1994, 27, 435.

8 A. L. Spek, *Acta Crystallogr. Sect. A: Found. Crystallogr.*, 1990, A46, C34.